CARMA Memorandum Series #37

Bandpass calibration at 3mm wavelength

Murad Hamidouche, Athol Kemball
University of Illinois at Urbana-Champaign

November 22, 2006

ABSTRACT

This memo describes initial investigations of net bandpass determination methods for CARMA at 3mm wavelength using bright quasar calibrators. Temporal variability of the bandpass response over time-scales of both hours and days are described, and initial recommendations are made regarding bandpass calibration strategies for observers scheduling observations at 3mm wavelength using CARMA.

Change Record

Revision	Date	Author	Sections/Pages Affected
	Remarks		
1.0	2006-Sep-08	M. Hamidouche, A. Kemball	
	First draft.		
1.1	2006-Oct-23	M. Hamidouche, A. Kemball	
	Modifications of first draft.		
2.0	2006-Nov-16	M. Hamidouche, A. Kemball	
	Second draft.		

1. Introduction

This memorandum considers the problem of bandpass (BP) calibration for CARMA at 3mm wavelength. Specifically, we consider the problem of observationally determining the composite bandpass response at each antenna in each correlated baseband spectral window. The composite bandpass response results from the net effect of all components in the signal path at each antenna. We consider only the determination of the total bandpass response for each observed baseband window in this memo, and do not factor it into constituent electronic or system contributions.

In this memo we describe the techniques of bandpass calibration we evaluated for CARMA at 3mm, summarize our results on bandpass variability, and make initial recommendations on best practice for observers scheduling observations in the 3mm band.

2. Bandpass calibration

We adopt a simple mathematical model for the visibility-plane data, incorporating antenna-based calibration corrections:

$$V_{mn}^{true}(\omega,t) = e^{j(\tau_n-\tau_m)\omega}\; G_m(t)G_n^*(t)\; B_m(\omega)B_n^*(\omega)\; V_{mn}^{obs}(\omega,t) \tag{1}$$

where $V_{mn}^{true,obs}(\omega,t)$ are the true and observed visibility cross-power spectra on baseline mn at time t over frequency ω, τ_m is the post-correlation residual group-delay for antenna m, $G_m(t)$ is the complex gain correction $g_m(t)e^{j\phi_m(t)}$ at antenna m, and $B_m(\omega)$ is the composite bandpass response at antenna m. Note that, in this model, the gain term $G_m(t)$ is assumed to have no frequency dependence, and the bandpass term, $B_m(\omega)$ is assumed to have no time dependence.

Bandpass solution strategies conventionally operate by solving for $B_m(\omega)$ using least-squares minimization of the residual norm:

$$\chi^2 = ||\; V_{mn}^{true}(\omega,t) - e^{j(\tau_n-\tau_m)\omega}\; G_m(t)G_n^*(t)\; B_m(\omega)B_n^*(\omega)\; V_{mn}^{obs}(\omega,t)\; || \tag{2}$$

Residual delays, τ_m, are typically corrected separately in earlier calibration. These delay τ introduce a phase slope of magnitude $\Delta\phi = 2\pi\;\Delta\nu\;\tau$ across a baseband bandwidth $\Delta\nu$. From the equation above, it is clear that an estimate of $V_{mn}^{true}(\omega,t)$ and $G_m(t)$ is required to be able to solve for $B_m(\omega)$. The true visibility model depends on the source used during bandpass calibration observations, typically either a noise source, planet, or bright, compact extra-galactic calibrator. The flux density scale does not need to be known for this term if bandpass normalization to unit mean ampitude and zero mean pahse is adopted. Several approaches exist for solving for the residual gain term G_m, including self-calibration, separate or simultaneous with bandpass calibration, as well as division by a frequency average taken across each observed visibility cross-power spectrum at each time sample t. As in all least-squares problems, proper weighting is important. In addition, different parametrizations are possible for the complex bandpass response, $B_m(\omega)$, including both channel-based sampling and polynomials over frequency.

3. Observations

Given that there is sufficient SNR for bandpass calibration on strong extra-galactic continuum sources at 3mm, we have used CARMA observations of strong quasars taken primarily for other commissioning tasks and science observations and re-used these for bandpass calibration evaluation. The observing blocks used in this analysis are enumerated in Table 1.

We have used these data to evaluate bandpass determination methods for CARMA at 3mm wavelength, as well as to investigate temporal bandpass variability on time-scales of days, weeks, and months.

Table 1. Observations used in this bandpass analysis.

Obsblock Date	Antenna Offline	Source	BW (MHz) Band 1, 2, & 3	LO (GHz)	Start. Freq. (GHz) Band 1, 2 & 3
3c273.2006aug20.2.mir 20 Aug 2006	3,8	3c273	500, 8, 500	95	92.46242, 93.24745 92.96242
ct006.fourSource.2006aug22.1.mir 22 Aug 2006	3,8	3c273, noise	500, 500, 500	95	92.46875, 93.46875 92.96875
ct002.3c273.2006aug24.1.mir 24 Aug 2006	3,8	3c273	500, 500, 500	95	92.45758, 93.45758 92.95758
RF_test.3c273.2006aug28.1.mir 28 Aug 2006	2,3,8,15	3c273	500, 500, 500	95	92.46875, 93.46875 92.96875
ct002.array_sys.2006aug30.1.mir 30 Aug 2006	3,8	3c273	500, 500, 500	95	92.46875, 93.46875 92.96875
cx005.clsBmap.2006sep09.1.mir 09 Sep 2006	3	3c273	500, 500, 500	95	92.46875, 93.46875 92.96875
base.comb.2006sep20.2.mir 20 Sep 2006	1,3	3c454.3	500, 500, 500	95	92.46875, 93.46875 92.96875
base.test.2006oct12.1.mir 12 Oct 2006	1,3	3c273, noise + strong quasars	500, 500, 500	95	92.46875, 93.46875 92.96875
bandpass.3C273.2006oct20.1.mir 20 Oct 2006 (Continuum)	3	noise	500, 500, 500	95	92.46875, 93.46875 92.96875
bandpass.3C273.2006oct20.1.mir 20 Oct 2006 (Sp Line.)	1,3	3c273, noise	500, 8, 8	95	92.46875, 93.25378 92.75378
bandpass.3C345.2006oct21.1.mir 21 Oct 2006 (Continuum)	1,3	3c345, noise	500, 500, 500	95	92.46875, 93.25378 92.75378
bandpass.3C345.2006oct21.1.mir 21 Oct 2006 (Sp Line.)	1,3	3c345, noise	500, 8, 8	95	92.46875, 93.25378 92.75378

4. Data reduction and analysis

4.1. Delay calibration

The antenna-based delays can be deduced by solving for the delays using the Miriad task *mfcal* with the additional option of 'delay'.

Correcting for the delays is usually done by observing a strong quasar (e.g. 3c273 or 3c454.3) in continuum mode at transit, so the observations are not affected by any baseline errors. Or, one can observe the noise source introduced before the correlators in the CARMA signal path. Then, we can vary the delays until we obtain a ≈0 phase slope over frequency. Plotting the phase versus channels[1] provides an easy way to estimate the delay errors using equation 2. Of course, the delays are antenna-based but the plots are for each pair of antennas, so a reference antenna needs to be chosen for the array (usually CARMA 1). An improved estimate of the phase slope is possible across both sidebands of each band jointly. The delay in ns in this case is given as:

$$\tau = 1/360 \times signUsb \times (|slopeUSB| + |slopeLSB|)/2 \times NCHAN \times BW[GHz]/1GHz \tag{3}$$

where $slopeUSB$ is the slope of the phase in degrees per channel in the upper sideband ($slopeLSB$ in the lower sideband), and $signUSB$ is the sign of $slopeUSB$. The values $slopeUSB$ and $slopeLSB$ are expected to have the same absolute values with different signs; however this is usually not exactly the case.BW is the single-sideband (SSB) bandwidth in GHz and $NCHAN$ is the number of channels (typically 15 for a BW = 0.5 GHz).

For example, from the observations of 3c273 on 22 August 2006 (see Table 1), we deduced a delay error of 0.77 ns for CARMA 14 and 0.44 ns for CARMA 15. The reference antenna was CARMA 1. These delay errors can be removed directly on-line using the subarray routine *updateDelays*.

4.2. Bandpass Calibration Methods

We have evaluated standard bandpass calibration methods as implemented in Miriad tasks *mfcal* and *smamfcal*[2] for the task of determining the net 3mm bandpass response in each observed spectral window using bright compact quasar calibrators. The task *mfcal* solves for the bandpass response per frequency channel across each spectral window (i.e. in discrete, sampled form), while simultaneously solving for the phase correction over time. The SMA task *smamfcal* is modeled after *mfcal* but allows solution for a polynomial bandpass over frequency and supports additional weighting schemes. In *smamfcal*, the data are weighted by

---

[1] In MIRIAD using the *uvspec* task.

[2] For more details on *smamfcal* see the SMA bandpass report at http://smadata.cfa.harvard.edu/miriadWWW/smaspec /bptest/bpass_tst.html

the inverse of $< amplitude > /\sigma^{2x}$, where σ is the rms noise of a visibility V_{mn} and $< amplitude >$ is the amplitude of the average of $V_{mn}(\omega, t)$.

For a specific test, we have used the observing block bandpass.3C273.2006oct20.1.mir (see Table 1 for details on this observation) toward 3c273. In these data, the correlator was configured to a bandwidth of 500 MHz for all bands then switched in the middle of the track into 8 MHz for band 2 and 3. We use only band 2 and 3 here. We solve for the BP using all the combinations of the weighting factor, x=-1,1,2,3 with: 1) channel-based bandpass solution (*mfcal*), and 2) a polynomial bandpass (*smamfcal*) of order n, where n=1, 2, 3, 4, 5, and 10 in the case of BW = 8 MHz in order to reduce the number of free parameters. The bandpass solution shapes are consistent in all cases for both phase and amplitude. Derived bandpass solutions for the 500 MHz data obtained for this observing block are shown in Figures 1-4.

To quantify the efficiency of each method, we calculate variability statistics across frequency for the corrected visibilities on each baseline relative to the reference antenna CARMA 4 (which has the lowest system temperature). We calculate the peak-to-peak value of the amplitude of the corrected visibility cross-power spectra over frequency and normalize it by the amplitude mean value $(MAX_{amp} - MIN_{amp})/ < Amplitude >$ $\times 100$. For the phase, we just calculate the peak-to-peak value $(MAX_{ph} - MIN_{ph})$ in degrees. We compare the median of these values across each baseline to the reference antenna (CARMA 4) for all the visibilities, and show the results in Table 2 for BW=500 MHz, and in Table 3 for BW=8 MHz.

We see in Table 2 (at BW = 500 MHz) that the lowest values $< 15\%$ in amplitude and < 10 deg in phase are obtained using *mfcal* or *smamfcal* with a channel-based (non-polynomial) bandpass solution. We find the best values, a variation $< 10\%$ in amplitude and < 10 deg in phase, by solving on a channel-by-channel basis using the task *mfcal* (see Figure 1 and 2).

We see in Table 3 for BW = 8 MHz that there is no significant trend in bandpass solution quality over the solution parameters. The lowest peak-to-peak values in amplitude and phase are $> 39\%$ and > 20 deg respectively. The lowest values are obtained using the task *mfcal*. Figure 5-8 show examples of the solutions obtained at BW = 8 MHz.

Table 2. Median (over baseline) of peak-to-peak values of the calibrated phase and amplitude variation per sideband (band 2 and 3 only). The reference antenna is CARMA 4 and BW = 500 MHz, with 15 channels per sideband.

Task	*Weight*	*Polynomial*	AMPLITUDE (%)		PHASE (deg)	
	(x)	(n)	USB 2	USB 3	USB 2	USB 3
Raw Data	-	-	56.8977	112.582	42.1690	31.9840
selfcal	-	-	56.4632	111.872	42.0631	31.8280
Mfcal	-1	No	5.21645	5.37552	2.05874	3.14924
Smamfcal	-1	No	4.49979	4.92168	2.00401	3.13589
Smamfcal	1	No	5.25381	12.2914	1.86354	3.19510
Smamfcal	2	No	6.04482	10.8816	3.14861	5.65833
Smamfcal	3	No	9.89139	13.6978	4.72881	7.60195
Smamfcal	-1	Yes (1)	50.2520	42.2074	14.1550	16.6506
Smamfcal	1	Yes (1)	50.7068	43.7045	16.0594	16.9835
Smamfcal	2	Yes (1)	50.7725	42.4905	16.0736	16.6565
Smamfcal	3	Yes (1)	49.3019	44.4341	17.7266	17.4002
Smamfcal	-1	Yes (2)	26.2632	39.1156	12.5711	13.4024
Smamfcal	1	Yes (2)	27.0191	41.3490	15.2303	13.3657
Smamfcal	2	Yes (2)	26.3976	38.6486	13.0253	15.3836
Smamfcal	3	Yes (2)	26.1160	39.0248	12.5908	15.8142
Smamfcal	-1	Yes (3)	25.1275	22.8795	9.43420	12.9548
Smamfcal	1	Yes (3)	24.2411	32.2746	11.7761	13.3682
Smamfcal	2	Yes (3)	24.7146	22.0132	12.1131	13.9213
Smamfcal	3	Yes (3)	25.2444	28.3800	10.2307	13.6847
Smamfcal	-1	Yes (4)	22.3072	16.2024	8.30474	8.03081
Smamfcal	1	Yes (4)	22.3528	26.5335	10.1104	8.13699
Smamfcal	2	Yes (4)	22.2395	18.7743	10.5993	11.9149
Smamfcal	3	Yes (4)	22.7897	23.6039	9.27811	9.96950
Smamfcal	-1	Yes (5)	17.5783	13.8845	7.33243	6.29494
Smamfcal	1	Yes (5)	17.3127	19.3748	8.88350	6.21730
Smamfcal	2	Yes (5)	18.8313	16.8373	9.77699	9.27921
Smamfcal	3	Yes (5)	17.9583	18.9877	8.36847	8.60361

Table 3. Median (over baseline) of peak-to-peak values of the phase and amplitude variation per sideband (band 2 and 3 only). The reference antenna is CARMA 4 and BW = 8 MHz, with 63 channels per sideband.

Task	*Weight* (x)	*Polynomial* (n)	AMPLITUDE (%) USB 2	USB 3	PHASE (deg) USB 2	USB 3
Raw Data	-	-	54.9806	70.1811	30.9445	33.0647
selfcal	-	-	47.9005	58.7425	27.9709	40.8300
Mfcal	-1	No	39.0244	64.5613	20.5283	30.4953
Smamfcal	-1	No	39.7122	53.3994	20.9048	37.3432
Smamfcal	1	No	40.1929	53.2740	20.6427	28.2920
Smamfcal	2	No	86.6685	107.876	39.0945	49.9769
Smamfcal	3	No	81.0448	109.275	46.9284	53.9140
Smamfcal	-1	Yes (1)	46.9688	57.7232	29.1370	40.6974
Smamfcal	1	Yes (1)	45.4749	54.4108	31.9653	37.7911
Smamfcal	2	Yes (1)	46.6294	57.2961	33.5430	41.0333
Smamfcal	3	Yes (1)	46.3433	57.9535	32.9284	41.1983
Smamfcal	-1	Yes (2)	49.1820	60.2508	30.9790	40.6224
Smamfcal	1	Yes (2)	46.6046	55.0194	33.1457	40.4078
Smamfcal	2	Yes (2)	52.7827	58.3350	36.0501	41.1263
Smamfcal	3	Yes (2)	51.5614	59.5630	35.1347	41.3409
Smamfcal	-1	Yes (4)	46.4059	58.3906	29.0538	41.2477
Smamfcal	1	Yes (4)	46.8090	55.2765	29.6259	39.0704
Smamfcal	2	Yes (4)	56.9850	68.7594	34.3023	42.6915
Smamfcal	3	Yes (4)	54.1795	66.4798	33.7923	40.2501
Smamfcal	-1	Yes (5)	48.0080	58.2406	29.4089	41.1765
Smamfcal	1	Yes (5)	46.5932	55.7356	29.3552	37.6736
Smamfcal	2	Yes (5)	59.5339	71.3222	33.8655	43.3996
Smamfcal	3	Yes (5)	52.7405	73.6580	33.0875	41.3609
Smamfcal	-1	Yes (10)	51.2000	59.5387	29.1757	44.2985
Smamfcal	1	Yes (10)	45.8344	53.6376	30.2507	35.1397
Smamfcal	2	Yes (10)	65.8176	69.6075	37.2917	46.7237
Smamfcal	3	Yes (10)	55.7075	71.0876	37.4012	43.8106

As a further test of the effectiveness of bandpass solution methods, we have mapped[3] 3C273 after solving for the bandpass solutions using each of the methods above. Our results show that using *mfcal* provides the best results than when using smamfcal or selfcal alone (Figure 9 & 10).

[3]We use the miriad commands *invert, clean*, and *restor*.

4.3. Bandpass Temporal Variations

4.3.1 BP variability over hours:

We probe here the temporal variation of the BP on short time-scales (over a few hours of observation).

Visibility variability: We examine the 4-hour track taken toward the quasar 3c273 on 20 Aug 2006 starting at 20:27 UT. The quasar was high enough in the sky, beginning at 44 deg elevation, transiting at 52 deg then reaching 42 deg elevation at the end of the track. For these observations, LO1 was 95 GHz. Band 3 had a bandwidth of 500 MHz (over 15 channels) at a frequency of 92.96 GHz and band 2 had a bandwidth of 8 MHz (over 63 channels) at a frequency of 93.24 GHz. System temperatures were good and antennas 3 and 8 were off-line. CARMA 1 was used as a reference antenna in this test. We do not discuss band 1 here as it was not available on all antennas.

Figure 11 and 12 display the temporal variation of the visibilities on each baseline to the reference antenna, CARMA 1 . We show in these plots the temporal variation of the RMS_{band} over frequency for each of the three bands in both amplitude and in phase. A *crude* estimate of this temporal variation can be obtained from their modulation index (*rms/mean*) over the 4 hours of observations. Table 4 displays the modulation indexes of the amplitude and phase *RMS*s of Figure 11 and 12. We can directly deduce the temporal behavior of the frequency dependence per band from these indexes.

Band 2 (8 MHz over 63 channels): In amplitude, they seem stable over the 4 hours with an index not exceeding $\sim$ 57%. The lowest variability index, is found for the baseline 1-14 with a value of $\sim$ 13%. The phases are also relatively stable for most baselines. However, some baselines have a quite high indexes due to the sudden phase changes such as in the baseline 1-4.

Band 3 (500 MHz over 15 channels): In amplitude, the modulation indexes are generally better than band 2 (mostly $<$ 20%). In phase, there is similar behaviour to that in band 2.

Table 4. Modulation index of the amplitude and phase of the visibilities per baseline of bands 2 and 3.

	AMPLITUDE		PHASE	
Baseline	DSB2	DSB 3	DSB2	DSB 3
1-2	0.414792	0.156879	0.262196	0.171709
1-4	0.476769	0.127098	0.856306	0.405528
1-5	0.297248	0.113194	0.0981952	0.119333
1-6	0.475417	0.138580	0.0959557	0.117730
1-7	0.569900	0.296374	0.0640947	0.0564616
1-9	0.229132	0.0627517	0.329005	0.390268
1-10	0.249444	0.244831	0.0996271	0.0767994
1-11	0.249444	0.0820413	0.771371	0.683012
1-12	0.297248	0.186979	0.0588078	0.0822782
1-13	0.378542	0.147587	0.471779	0.544730
1-14	0.129023	0.119038	0.128205	0.0416236
1-15	0.512459	0.182422	0.103283	0.0902011

Bandpass solution variability: We further our investigation of the bandpass stability by comparing BP solutions determined within the track base.test.2006oct12.1.mir (see Table 1). The noise source was observed for several 5 min segments during this track. We compare the bandpass solutions of two 5 min noise source observations taken within this same track but 8 hours apart. We solved for the BP using the Miriad task *mfcal* that showed the best performance in the previous section. We compared the bandpass solutions in amplitude and phase by examining the variation of the amplitude ratio [Amp (Time 2)/ Amp (Time 1)] and the *RMS* of the phase difference [Phase (Time 2) - Phase (Time 1)]. These results are tabulated in Table 5. It is important to notice that we show in Table 5 the ***mean*** values of the amplitude ratios of the solutions across the bands from different obsblocks, as they quantify very well the amplitude temporal variation; and the ***RMS*** values of the phase difference of the solutions across the bands, as they quantify very well the phase temporal variations.

We plot the ratio of amplitude solutions and the difference of phase solutions between these two observations in Figure 13 and 14 respectively. Note, for the noise source, we only have data in the LSB. Figure 13 shows that the ratio of the amplitude solutions are very flat and are on average equal to 1.0$\pm$0.1 (Table 5); except CARMA 9, it has higher >1 solutions in band 2 and lower solutions <1 in band 3. The rms difference of the phase solutions are very stable across the bands (Figure 14). Their *RMS* values are mostly within 1 deg.

Table 5. **Mean** values of the ratios of the amplitude solutions and ***RMS*** values of the difference of the phase solutions across the LSB of bands 1, 2 and 3. This compares bandpass solutions for two data segments on the noise source separate by 8 hours.

	LSB 1		LSB 2		LSB 3	
Antenna	Amp Ratio mean±RMS	Phase diff. RMS deg	Amp Ratio mean±RMS	Phase diff. RMS deg	Amp ratio mean±RMS	Phase diff. RMS deg
C 1	1.00 ± 0.00	0.00	1.02 ± 0.00	0.00	0.99 ± 0.00	0.00
C 2	-	-	1.00 ± 0.00	0.44	1.00 ± 0.00	0.40
C 3	-	-	-	-	-	-
C 4	1.01 ± 0.00	0.65	1.01 ± 0.00	0.23	1.00 ± 0.00	0.88
C 5	1.00 ± 0.00	0.28	1.01 ± 0.00	0.09	0.99 ± 0.00	0.30
C 6	1.00 ± 0.00	0.96	1.00 ± 0.00	0.08	-	-
C 7	1.00 ± 0.00	0.36	1.00 ± 0.00	0.03	1.00 ± 0.00	0.22
C 8	-	-	1.00 ± 0.00	0.31	1.00 ± 0.00	0.69
C 9	-	-	1.22 ± 0.00	0.04	0.63 ± 0.00	0.41
C10	-	-	1.01 ± 0.00	0.26	0.99 ± 0.00	0.72
C11	-	-	1.00 ± 0.00	0.04	1.00 ± 0.00	0.27
C12	-	-	1.00 ± 0.00	0.27	1.00 ± 0.00	0.80
C13	-	-	0.99 ± 0.00	0.10	1.01 ± 0.00	0.20
C14	-	-	1.00 ± 0.00	0.06	1.00 ± 0.00	4.97
C15	-	-	1.00 ± 0.00	0.06	1.00 ± 0.00	0.08

4.3.2 BP variability over days or weeks:

We investigate here the BP variation over longer timescales of days or weeks. We compare the BP solutions obtained from datasets on different days to analyse their temporal behavior. We use the continuum datasets taken toward the quasars 3c273 and 3c454.3 on 09 Sept 2006, 20 Sept 2006, and 20 Oct 2006 (see Table 1 for details on these datasets).

We solve for the BP using the Miriad task *mfcal* and compare the bandpass solutions in both amplitude and phase between each pair of datasets. We analyse the BP variations by comparing the amplitude ratio (Amp Date1/ Amp Date2) and the rms of the phase difference (Phase Date1 - Phase Date2) between each pair of datasets. The results for the LSB of bands 1,2, and 3 are tabulated in Table 6.

1] Comparing 09 Sep 2006 & 20 Sep 2006 (11 days): The amplitude solutions of most antennas are stable within $<$ 5%, except CARMA 2 and 4 that vary more significantly in all bands. The absolute phase differences are mostly $<$ 20 deg. Band 3 has the most stable phases. CARMA 8 shows the highest variability of the phase rms over these 11 days in all bands. CARMA 7 shows a higher amplituded variability in band 1 only. On the other hand, overall CARMA 5 is the most stable in both phase and amplitude.

2] Comparing 20 Sep 2006 & 20 Oct 2006 (4 weeks): Similar to the previous comparison over 11 days, the amplitude solutions on most antennas are stable within $< 5\%$, except CARMA 2 and 4 that vary more significantly in all bands. Band 2 has the most stable phases. However, CARMA 8 shows an important variation of the rms phase over these 4 weeks in all bands. On the other hand, overall CARMA 13 is the most stable.

3] Comparing 09 Sep 2006 & 20 Oct 2006 (6 weeks): The amplitude solutions on all antennas are very stable within $< 5\%$. Overall the phases during this period are more stable than the previous two comparisons. CARMA 8 again shows the highest rms variation of the phase over these 6 weeks in all bands.

Table 6. **Mean** values of the ratios of the amplitude solutions and ***RMS*** values of the difference of the phase solutions across the LSB of bands 1, 2 and 3. Comparing two datasets taken at two separate calendar dates.

		LSB 1		LSB 2		LSB 3	
	Antenna	Amp Ratio mean±RMS	Phase diff. RMS deg	Amp Ratio mean±RMS	Phase diff. RMS deg	Amp ratio mean±RMS	Phase diff. RMS deg
09 Sept 2006 & 20 Sept 2006	C 2	1.18 ± 0.21	16.64	0.84 ± 0.03	7.87	0.84 ± 0.07	2.90
	C 4	1.28 ± 0.40	7.46	0.73 ± 0.04	10.03	0.61 ± 0.14	8.26
	C 5	1.01 ± 0.07	6.34	0.99 ± 0.01	11.99	0.98 ± 0.02	9.64
	C 6	0.98 ± 0.05	7.74	0.98 ± 0.02	12.50	0.98 ± 0.03	10.09
	C 7	0.85 ± 0.18	36.60	1.00 ± 0.01	12.30	0.98 ± 0.03	6.66
	C 8	0.94 ± 0.28	40.80	1.00 ± 0.01	60.12	0.98 ± 0.03	69.40
	C 9	-	-	0.98 ± 0.05	23.34	0.98 ± 0.10	8.38
	C10	-	-	1.00 ± 0.04	22.07	0.98 ± 0.08	19.00
	C12	-	-	1.00 ± 0.05	10.18	1.03 ± 0.16	10.81
	C13	-	-	0.98 ± 0.01	11.65	0.98 ± 0.02	9.69
	C14	-	-	0.99 ± 0.02	12.43	0.98 ± 0.02	8.77
	C15	-	-	0.98 ± 0.04	17.10	0.98 ± 0.03	5.62
20 Sept 2006 & 20 Oct 2006	C 2	0.87 ± 0.14	0.00	1.19 ± 0.04	0.00	1.19 ± 0.10	0.00
	C 4	0.89 ± 0.40	12.27	1.40 ± 0.08	7.08	1.64 ± 0.32	8.37
	C 5	0.95 ± 0.08	15.64	1.05 ± 0.01	6.38	1.02 ± 0.04	11.47
	C 6	1.02 ± 0.06	15.93	1.03 ± 0.02	2.66	0.99 ± 0.02	15.39
	C 7	1.28 ± 0.35	34.62	1.01 ± 0.01	6.59	1.01 ± 0.04	6.62
	C 8	1.29 ± 0.68	28.85	0.99 ± 0.01	76.24	1.00 ± 0.04	67.25
	C 9	-	-	1.01 ± 0.08	21.76	1.05 ± 0.13	10.24
	C10	-	-	1.00 ± 0.04	21.89	1.02 ± 0.09	27.29
	C12	-	-	1.01 ± 0.04	9.20	0.99 ± 0.14	20.08
	C13	-	-	1.01 ± 0.01	2.87	1.02 ± 0.02	12.06
	C14	-	-	1.02 ± 0.01	4.36	1.02 ± 0.03	32.34
	C15	-	-	1.01 ± 0.03	2.99	1.03 ± 0.03	45.25
09 Sept 2006 & 20 Oct 2006	C 2	1.00 ± 0.02	16.64	1.00 ± 0.01	7.87	0.99 ± 0.01	2.90
	C 4	1.00 ± 0.00	11.23	1.02 ± 0.00	3.78	0.97 ± 0.00	2.93
	C 5	0.96 ± 0.02	12.03	1.04 ± 0.00	6.06	1.00 ± 0.01	3.74
	C 6	1.00 ± 0.00	10.37	1.02 ± 0.00	10.83	0.97 ± 0.01	6.86
	C 7	1.04 ± 0.18	17.83	1.00 ± 0.01	6.21	0.99 ± 0.02	3.28
	C 8	1.07 ± 0.17	45.25	0.99 ± 0.01	40.02	0.98 ± 0.02	110.66
	C 9	-	-	0.99 ± 0.03	8.00	1.02 ± 0.02	4.12
	C10	-	-	1.00 ± 0.01	8.79	0.99 ± 0.02	10.30
	C12	-	-	1.01 ± 0.01	7.48	1.01 ± 0.02	10.41
	C13	-	-	0.99 ± 0.01	11.47	1.00 ± 0.01	4.41
	C14	-	-	1.01 ± 0.02	15.33	1.00 ± 0.02	34.54
	C15	-	-	0.99 ± 0.02	15.92	1.01 ± 0.01	43.49

5. Summary

• We investigated different approaches to solve for the net bandpass in each spectral window. For the high SNR case, a 500 MHz sideband over 15 channels, we found that solving for a channel-based bandpass response using Miriad tasks *mfcal* or *smamfcal* (in non-polynomial mode) provided a better solution over a polynomial bandpass fit. They both significantly reduce the peak-to-peak variability of the phase and amplitude of the corrected visibilities across the side-bands by more than a factor of $\sim$10 (see Table 2). For the lower SNR case, in an 8 MHz bandwidth over 63 channels, the channel-based sampling method (*mfcal* or *smamfcal*) still provides somewhat better results than the polynomial bandpass fit. However, the reduction in variability over frequency is not as clear as in the high-SNR 500 MHz case, as might be expected. Our overall experience is that channel-based bandpass solutions using *mfcal* is the best approach for bandpass calibration in the CARMA 3mm band.

• We find that the bandpass solutions over short timescales (hours), are stable within $<$ 5% in amplitude and within $\sim$1 deg in phase rms across the side-bands over intervals of 8 hours (see Table 5). We recommend observing a strong quasar (e.g. 3c273, 3c345, or 3c454.3) as a bandpass calibrator for a few minutes ($\sim$2 to 5 min) twice within a 6-8 hour track, at the beginning and at the end of the track.

• In an investigation of bandpass temporal variability over longer timescales of days or weeks, we found that: i) bandpass amplitude solutions are stable within $<$ 5% over 6 weeks for all antennas that were online at all bands; ii) bandpass phase rms is generally stable within $\sim$ 10 deg , but with higher variability found for CARMA 8, 14, and 15, and iii) band 1 bandpass solutions generally show a lower stability over time than bands 2 and 3.

6. Future work

Further work is needed in bandpass characterization for CARMA beyond this initial study, including: i) factorization of the bandpass response by dominant system contribution; ii) investigation of bandpass calibration using autocorrelation spectra; iii) frequency variability studies; iv) further time variability studies and time variability monitoring; and v) bandpass determination over the full set of CARMA window bandwidths.

Appendix

A. Miriad Tasks

We show in this section the Miriad commands and their parameters that were used in this analysis. We show the example of the dataset "bandpass.3C273.2006oct20.1.mir".

We split first the data to make a dataset file that contains only a BW = 500 MHz. The total observing time is about 40 min, sampled over $\sim$ 1.7 min record time. The source was rising between an elevation of 37 to 42 deg. System temperatures were very good and CARMA 1 and 3 were offline. We chose CARMA 4 as a reference antenna since it has a very good T_{sys}, all its receivers were working all the time, and it was among the antennas that were in the center of the array.

Split the data:

• uvcat vis=bandpass.3C273.2006oct20.1.mir out=3C273.2006oct20.500.mir
select=time(15:40,16:20)

Phase calibration:

• selfcal vis=3C273.2006oct20.500.mir interval=1.9
options=amp,apriori,noscale line=chan,90,1,1,1 refant=4

BP calibration using mfcal:

• mfcal vis=3C273.2006oct20.500.mir refant=4 interval=1.9 options=interpolate flux=12.73

mfcal can also solve for the delays with the options=delay. But we recommend to use the *updateDelays* routine (see §4.1).

BP calibration using smamfcal:

• smamfcal vis=3C273.2006oct20.500.mir refant=4 interval=1.9 weight=x
options=wrap,interpolate,opolyfit polyfit=n,0 flux=12.73

BP calibration using smamfcal with a polynomial fitting:

• smamfcal vis=3C273.2006oct20.500.mir refant=4 interval=1.9 weight=x
options=wrap,interpolate flux=12.73

In smamfcal, x = -1,1,2,3 and n = 1-10.

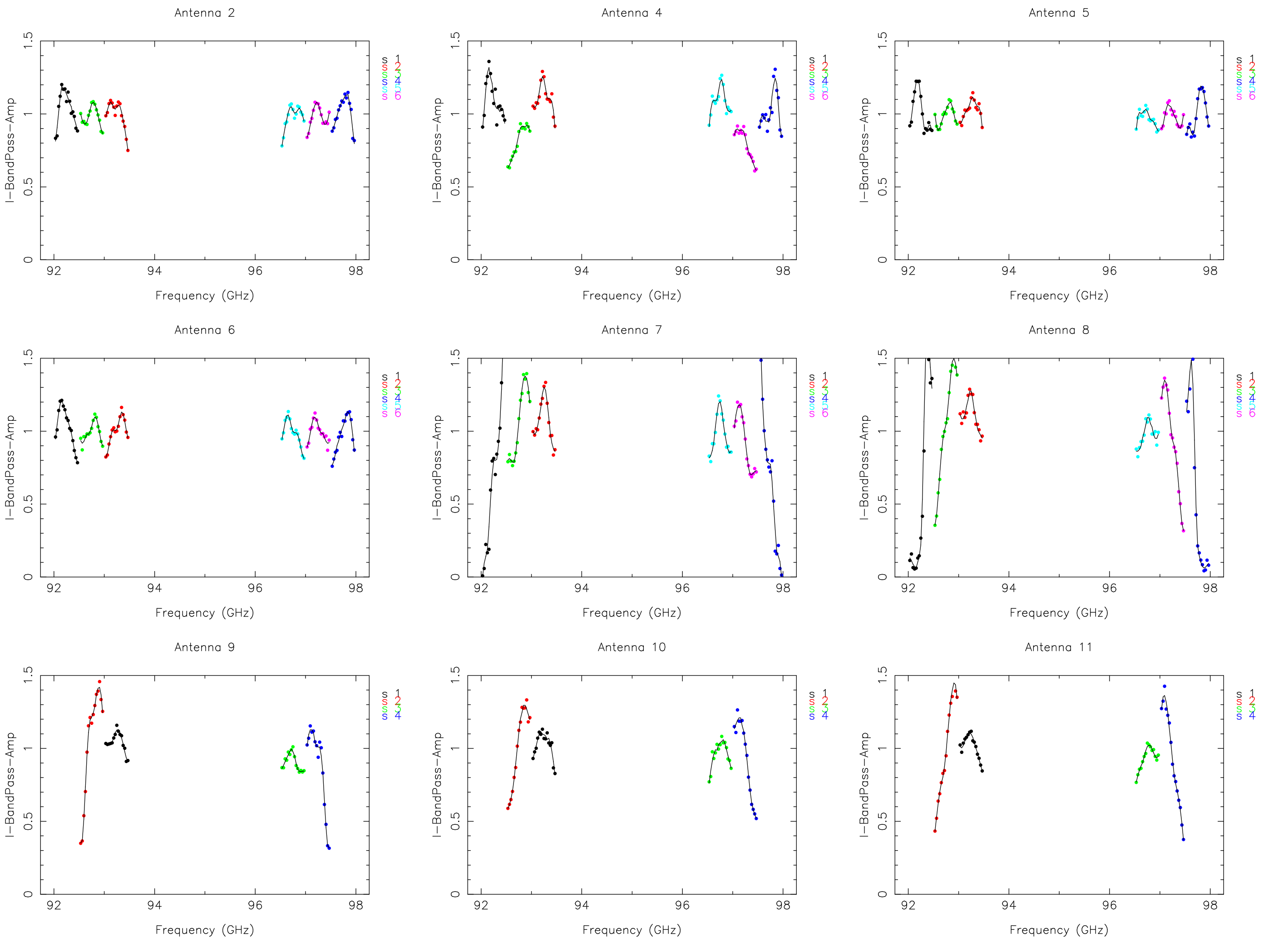

Fig. 1.— Example of nine antennas' amplitude solutions for 3c273 at 95 GHz with a BW = 500 MHz in all bands, and the reference antenna is CARMA 4. These solutions are obtained using *mfcal*.

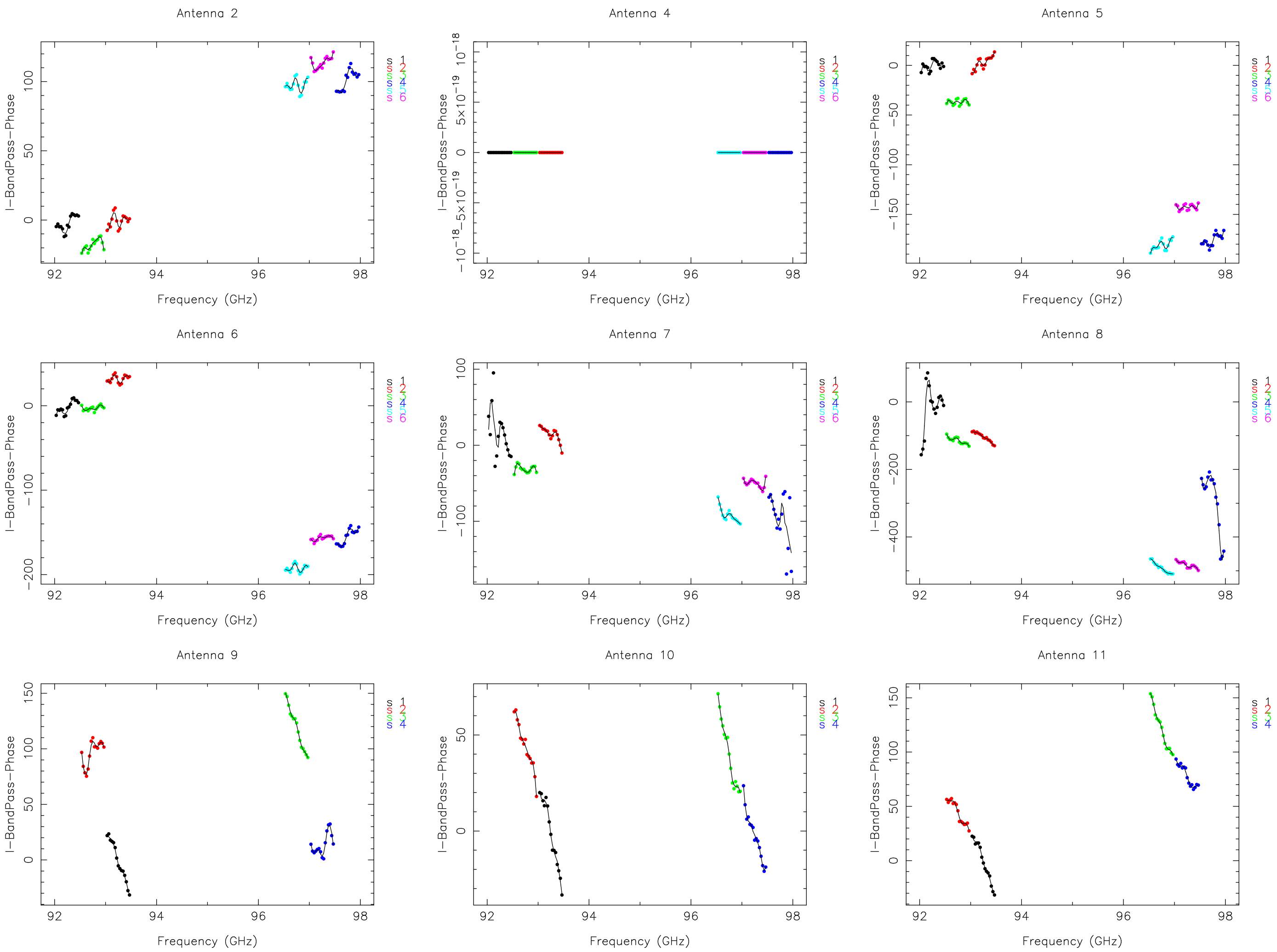

Fig. 2.— Same as Figure 1 for a phase solutions.

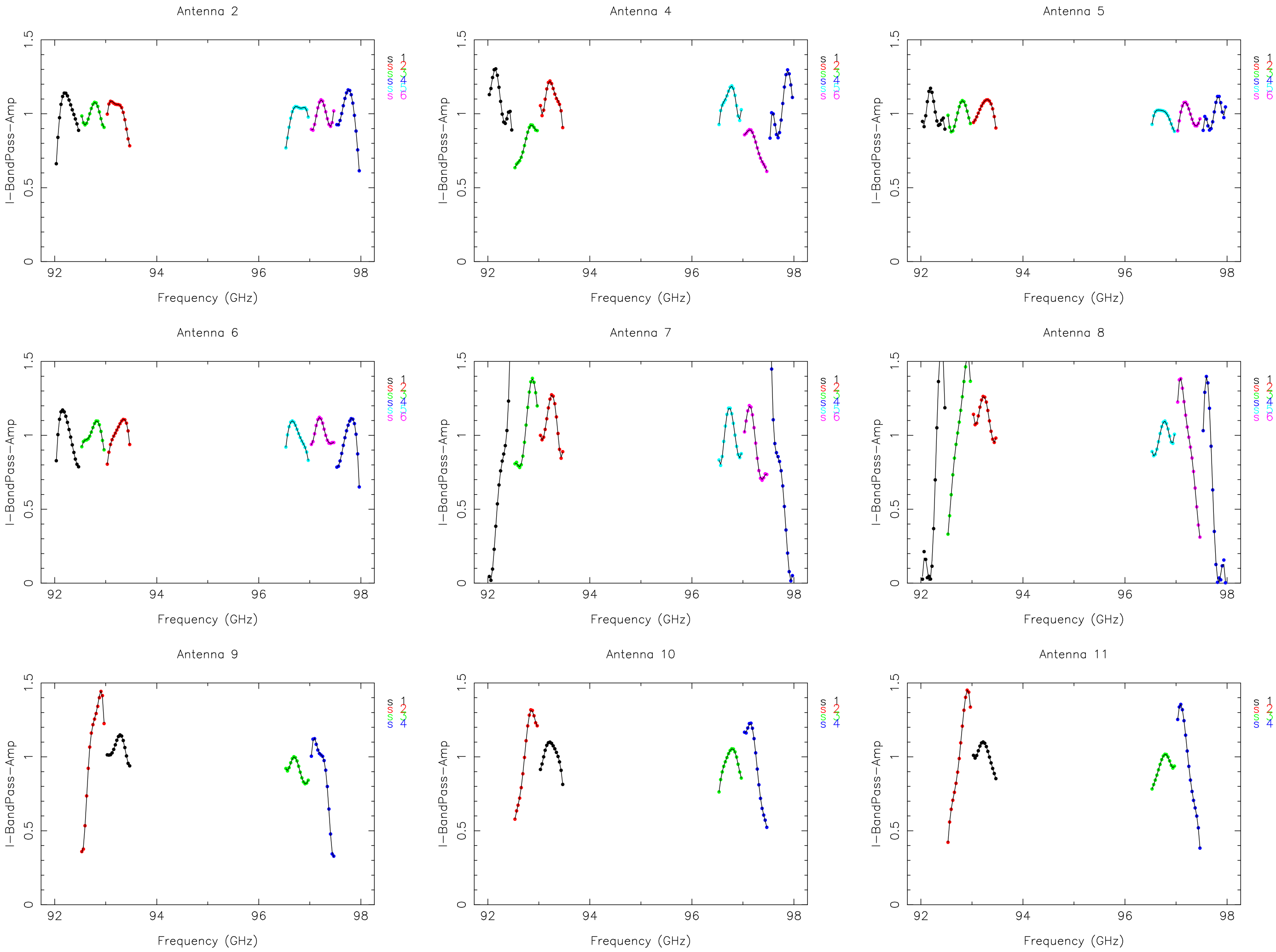

Fig. 3.— Example of nine antennas' amplitude solutions for 3c273 at 95 GHz with a BW = 500 MHz in all bands. These solutions are obtained using *smamfcal* by fitting a polynomial of the order 5 and a weight of 2.

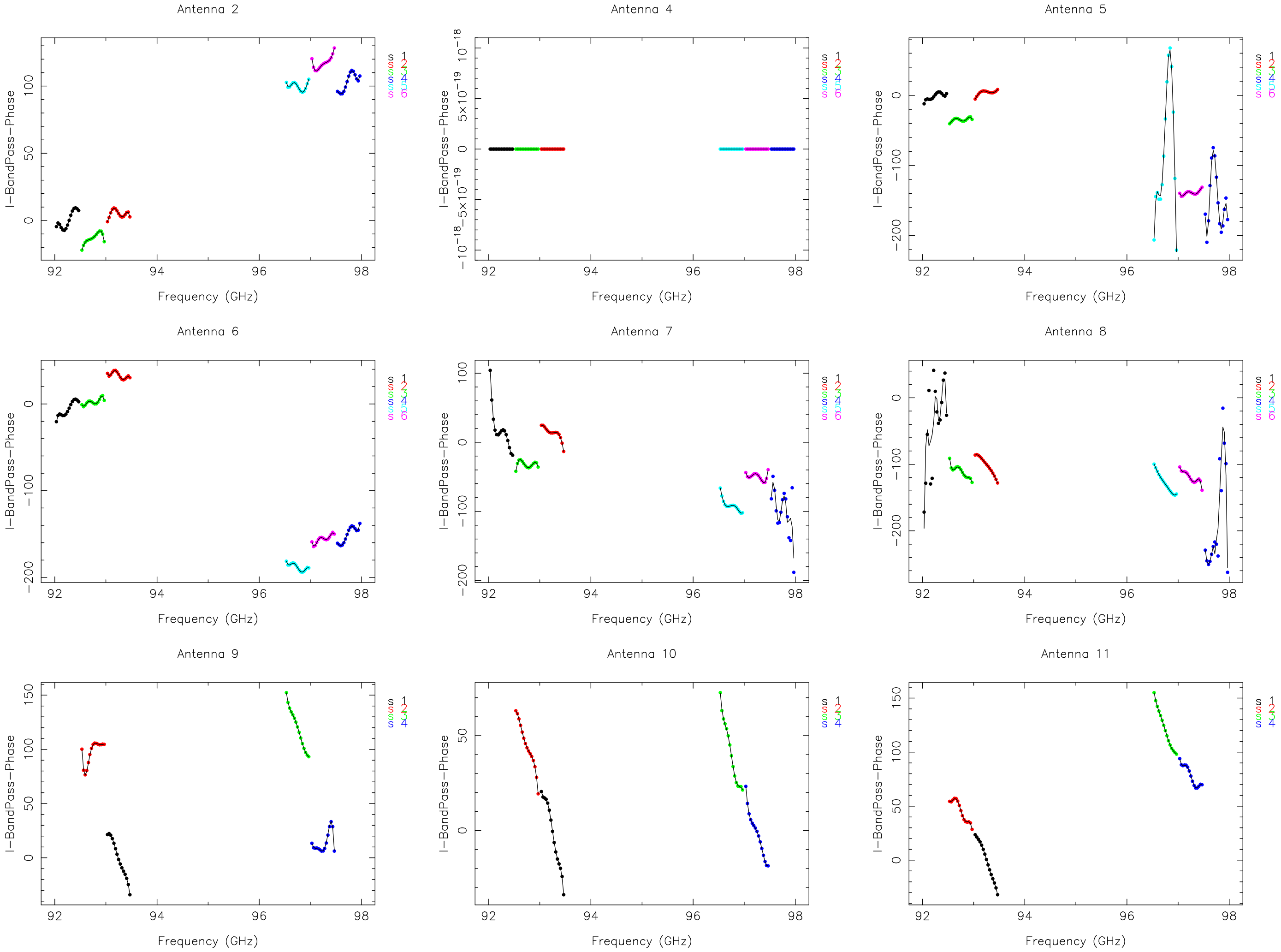

Fig. 4.— Same as Figure 3 for a phase solutions.

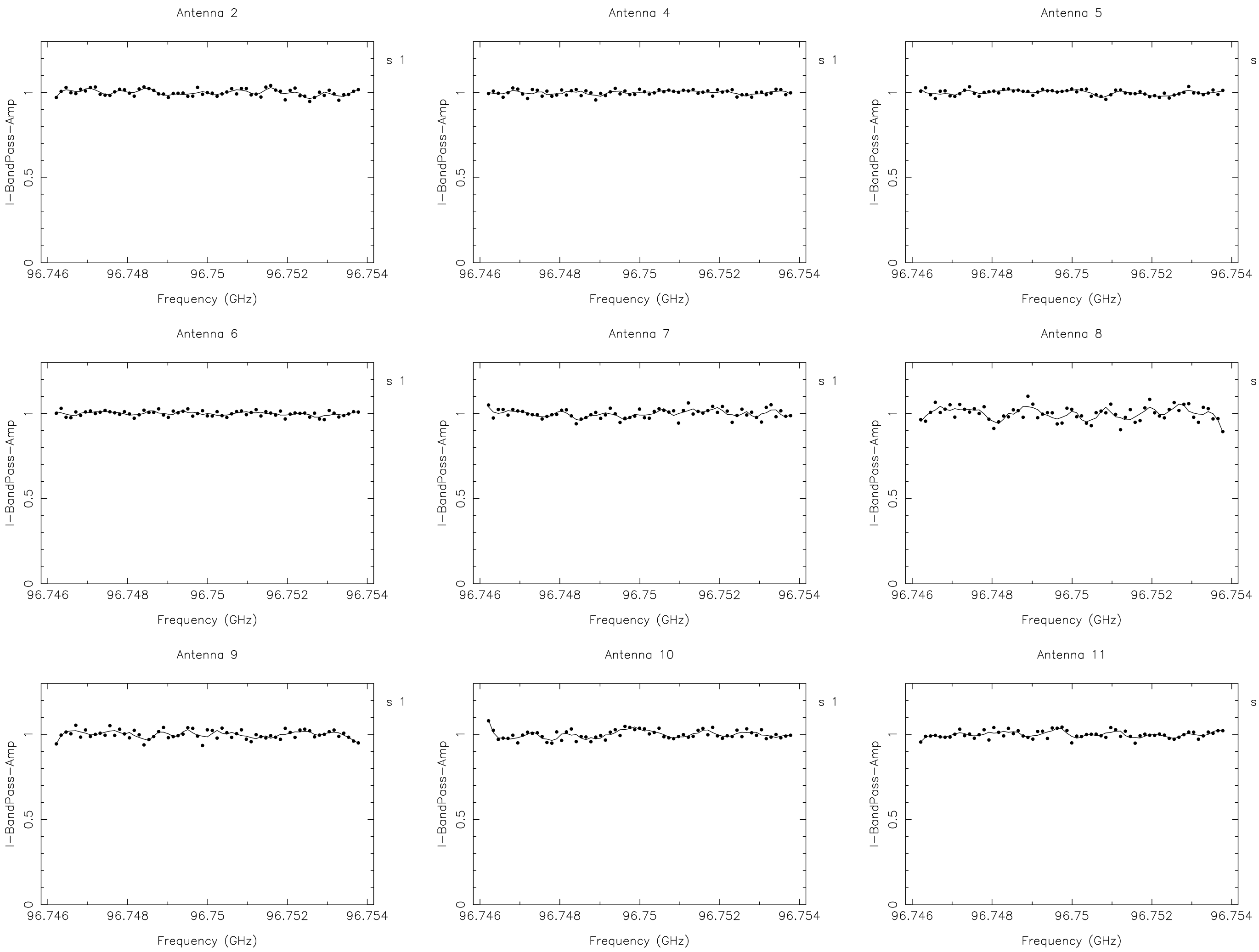

Fig. 5.— Example of nine antennas' amplitude solutions for 3c273 at 95 GHz with a BW = 8 MHz in Window 5 (USB 2) and the reference antenna is CARMA 4. These solutions are obtained using *mfcal*.

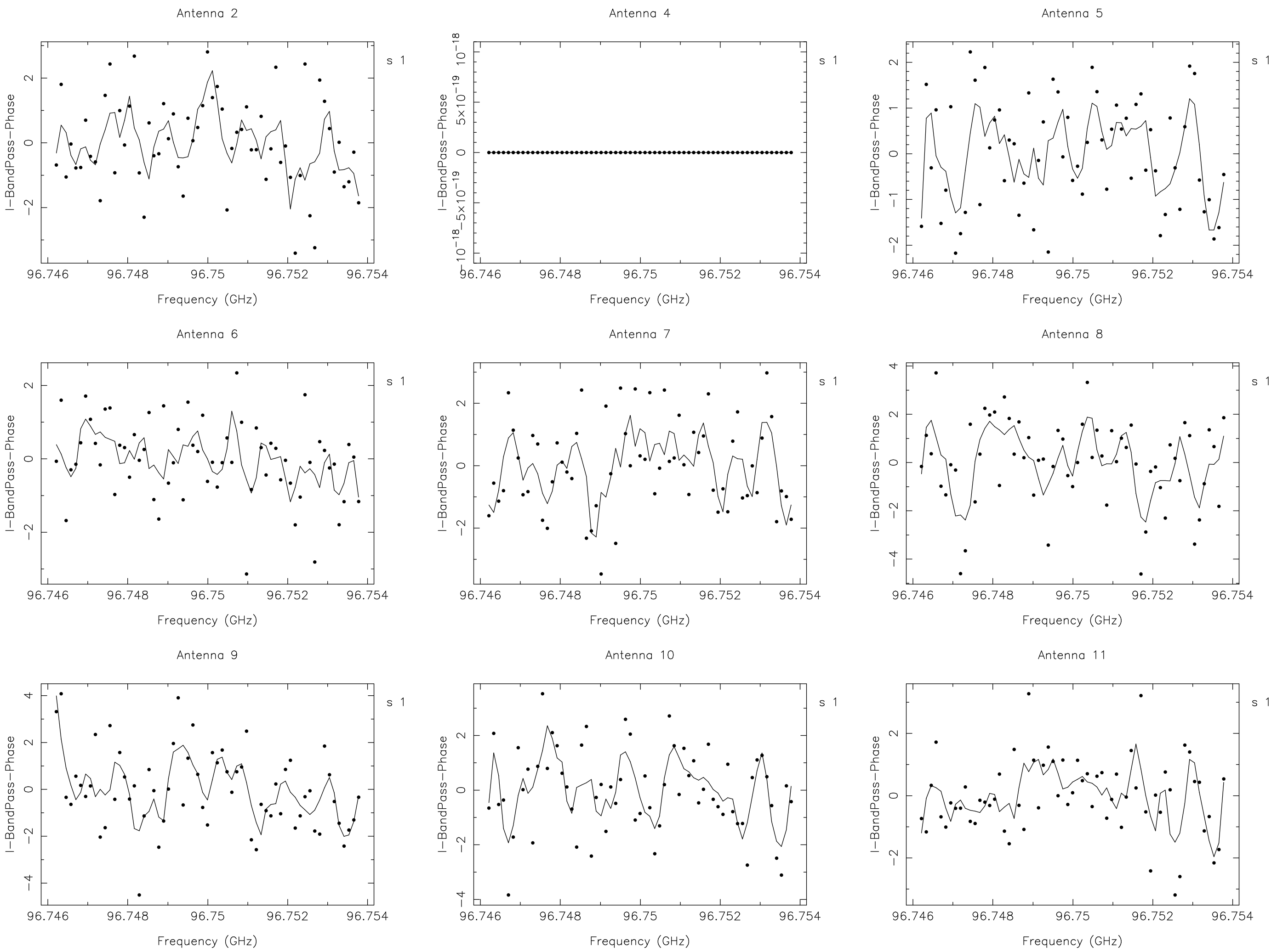

Fig. 6.— Same as Figure 5 for the phase solutions.

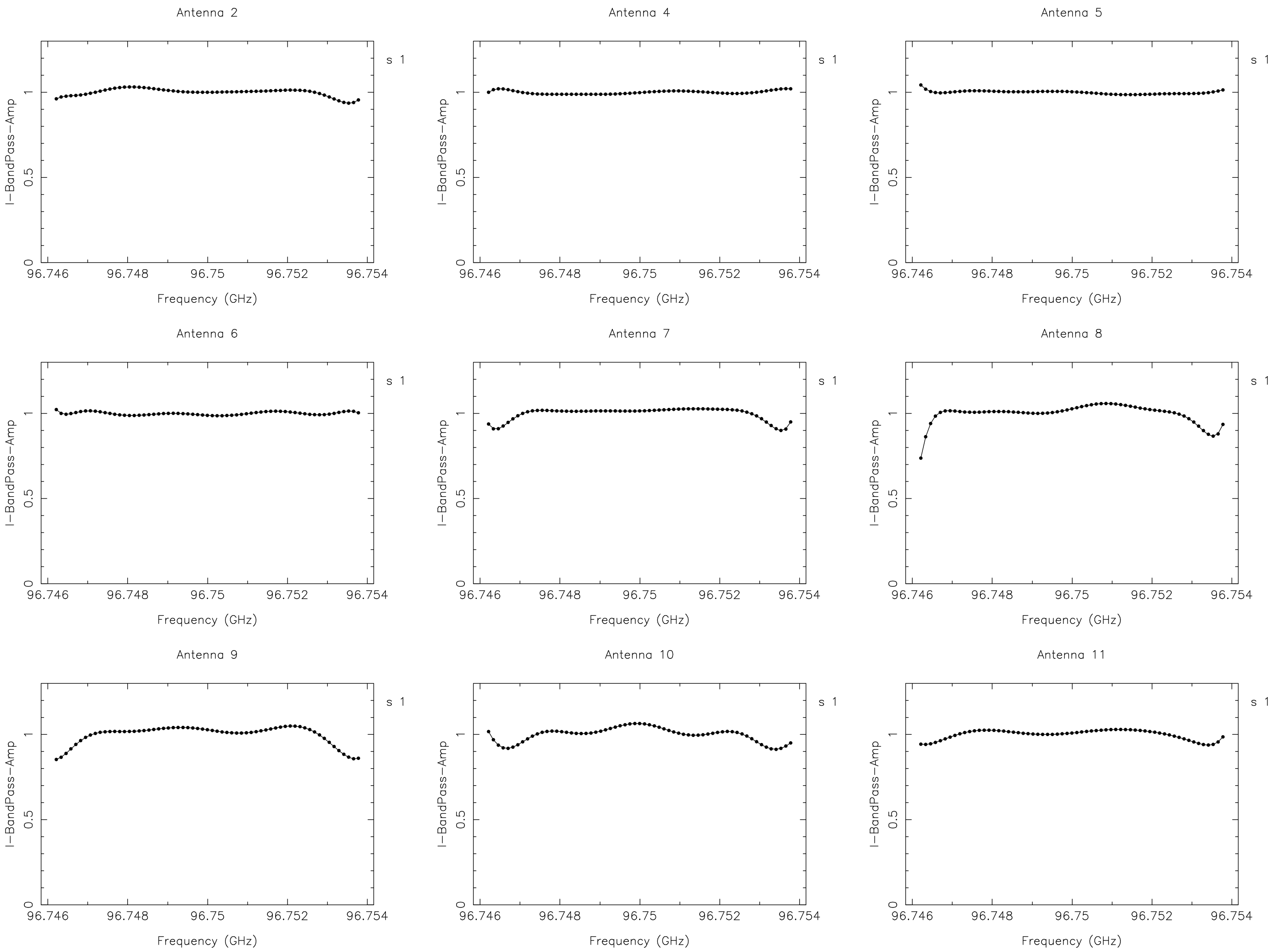

Fig. 7.— Example of nine antennas' amplitude solutions for 3c273 at 95 GHz with a BW = 8 MHz in Window 5 (USB 2). These solutions are obtained using *smamfcal* by fitting a polynomial of the order 10 and a weight of 1.

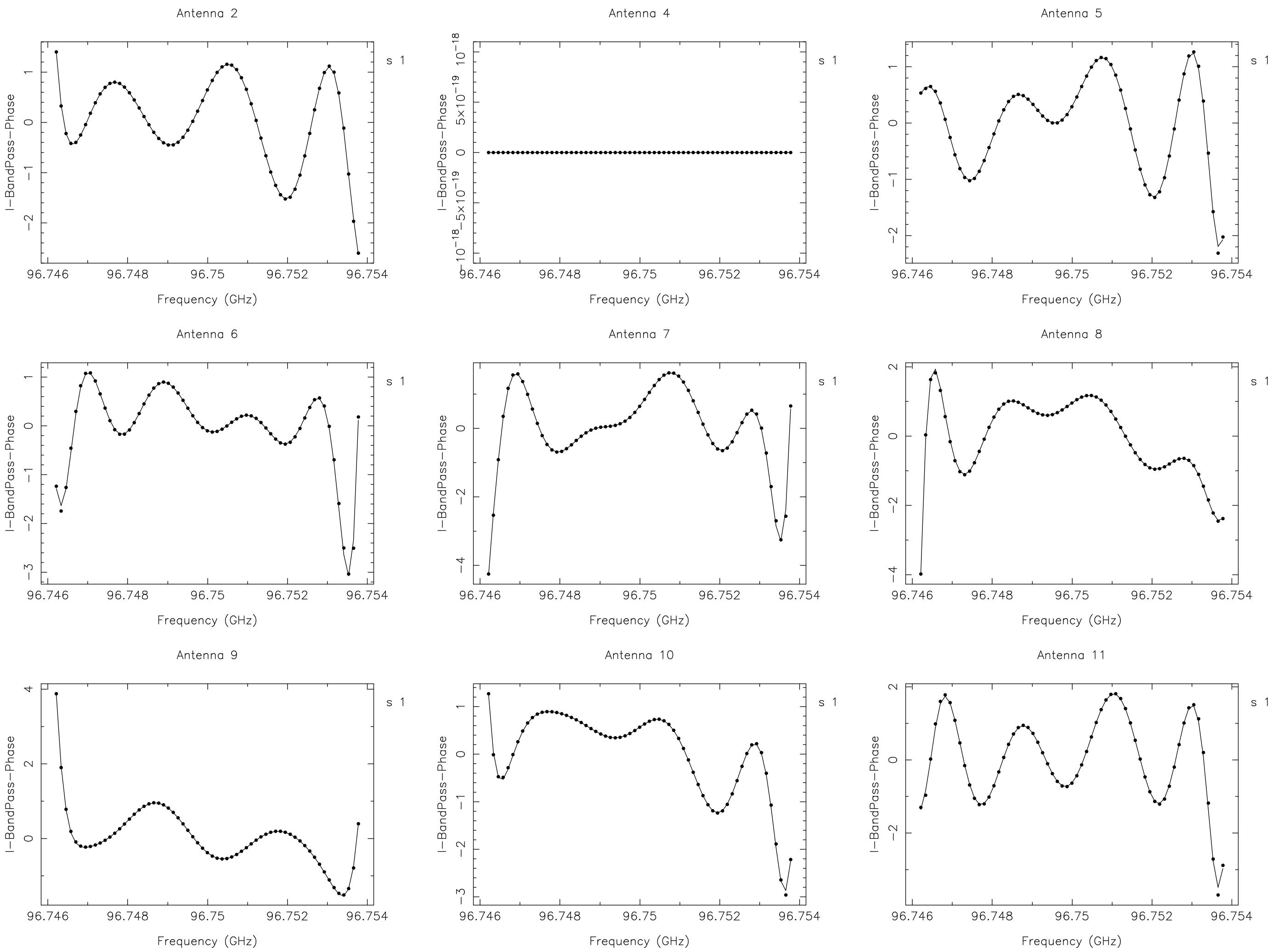

Fig. 8.— Same as Figure 7 for the phase solutions.

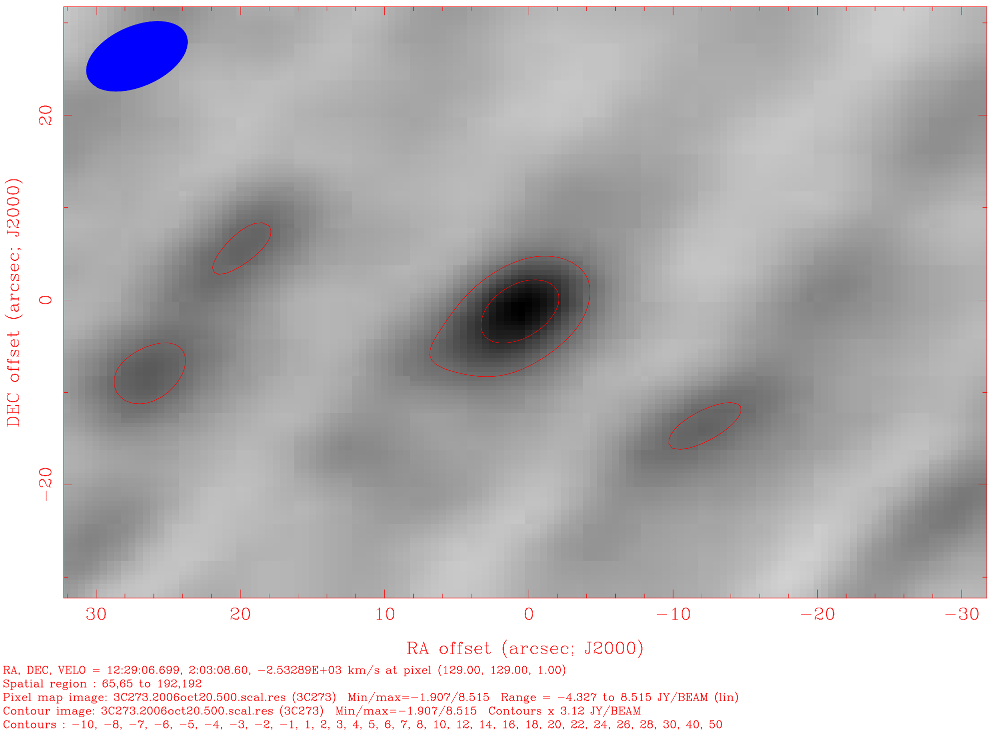

Fig. 9.— Map of 3c273 of window 2 only with a BW = 500 MHz. The dataset were reduced using selfcal only to solve for the gains. The total flux is 12.88 Jy. The contours are in steps of $\pm(1,2,3,4,5,6,7,8,10,12,14,16,18,20,22,24,26,28,30,40,50)\times\sigma$, where σ=3.12 Jy.

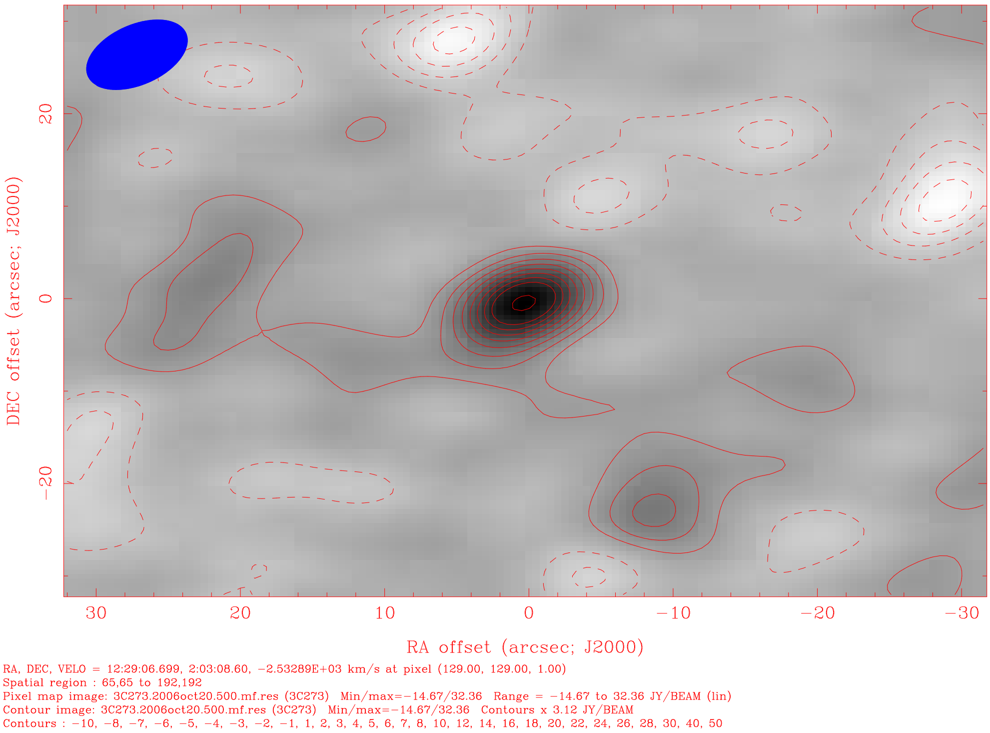

Fig. 10.— Same as the previous map but The dataset were reduced using selfcal and mfcal to solve for both the gains and the bandpass. The total flux is 33.57 Jy.

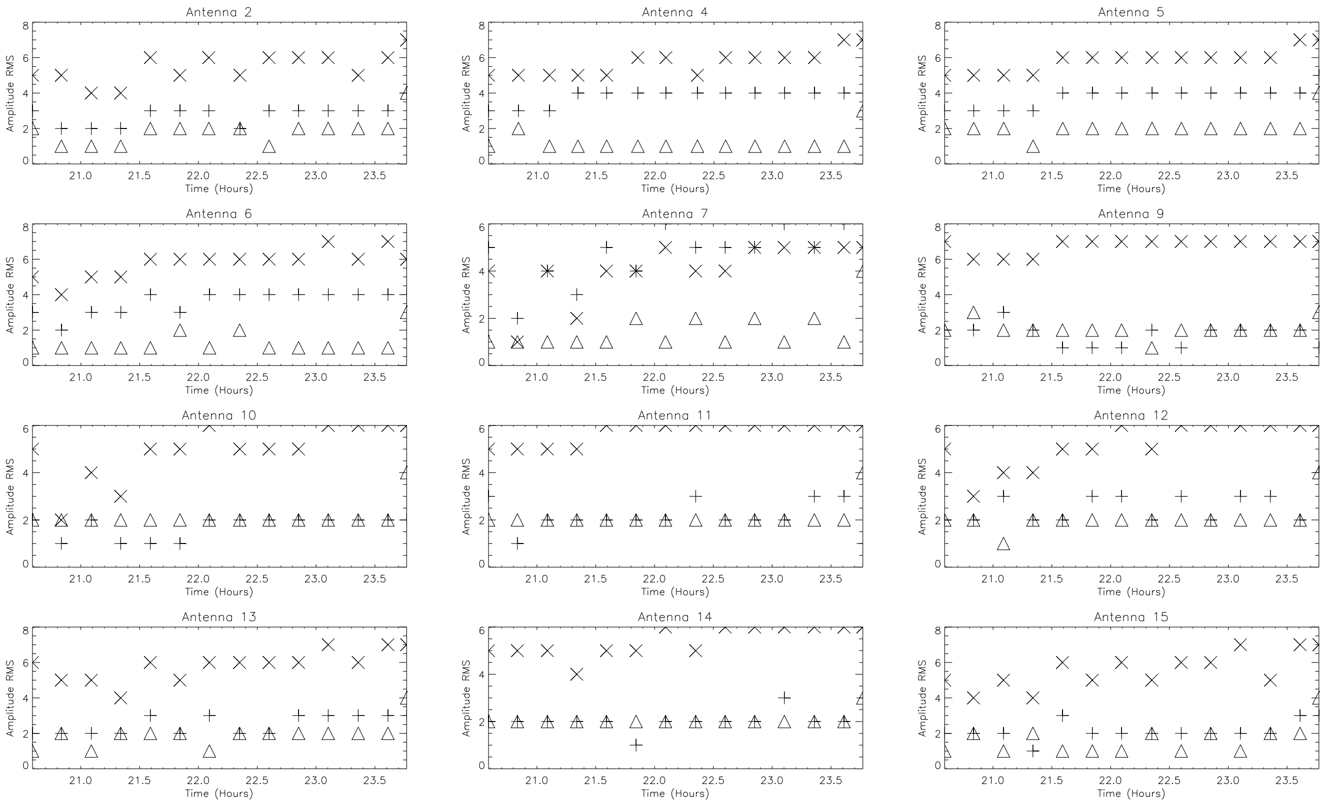

Fig. 11.— Temporal variation of the *rms*, across the bands, of the visibility amplitude over each baseline (+: Band 1, △: Band 2, ×: Band 3). CARMA 1 was the reference antenna. Each data point is an average over ∼10-14 minutes.

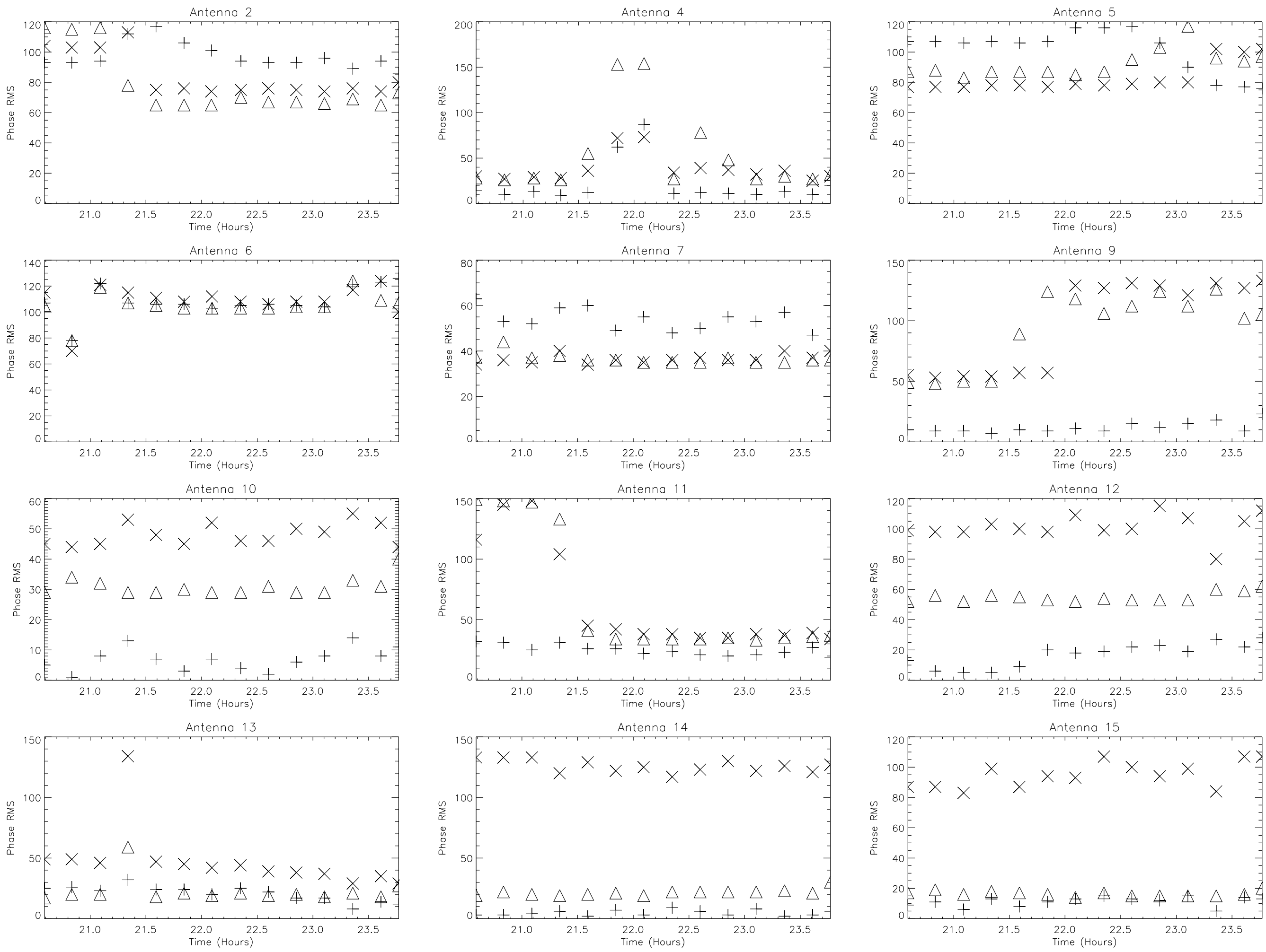

Fig. 12.— The same as Figure 10 for the visibility phase.

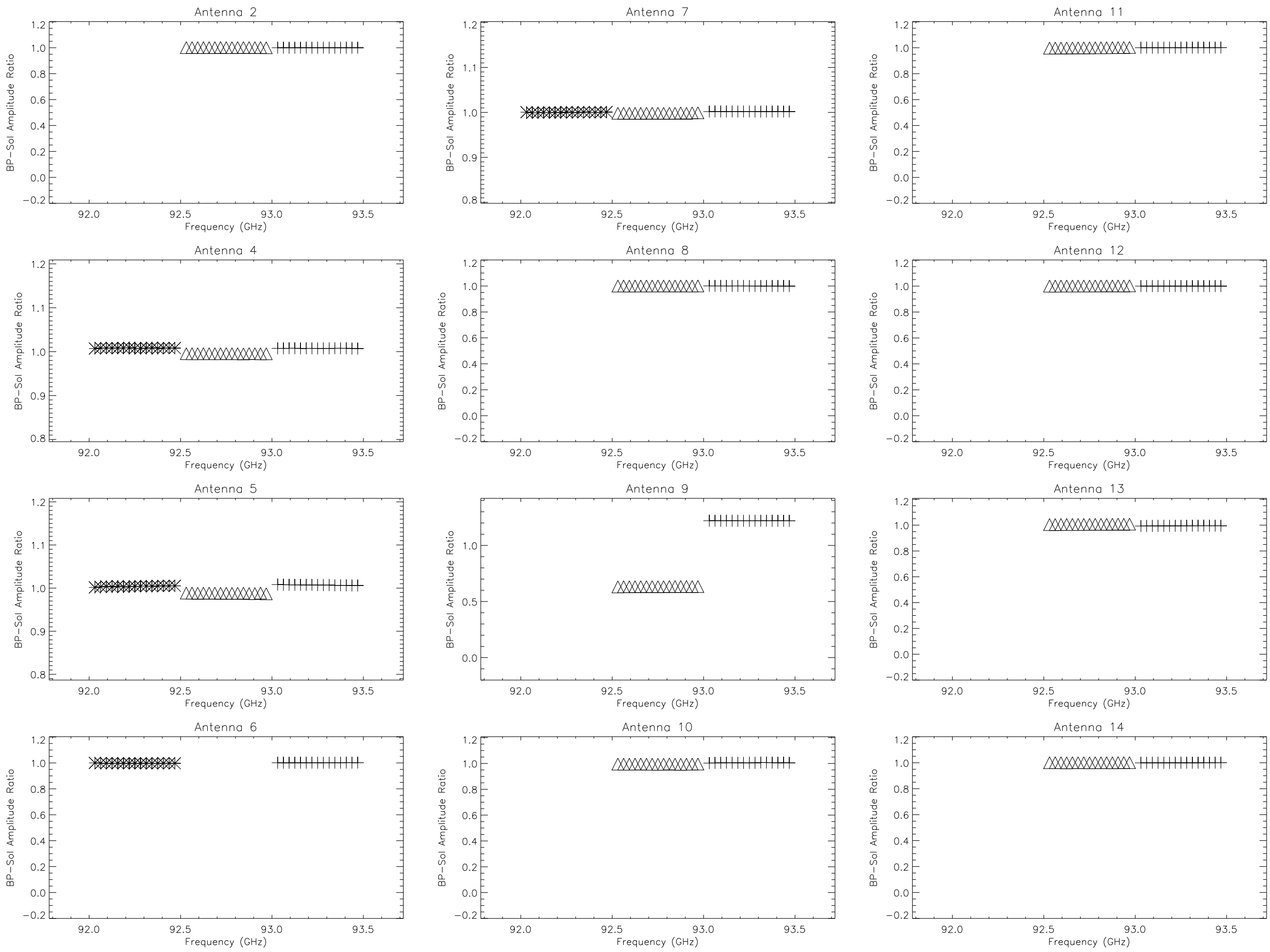

Fig. 13.— BP Solutions amplitude ratio between 2 dataset of the noise source taken 8 hours apart from each other. There are only the LSB windows in these dataset and all set at a BW = 500 MHz ($\times$: LSB 1, $+$: LSB 2, $\triangle$: LSB 3). CARMA 1 was the reference antenna.

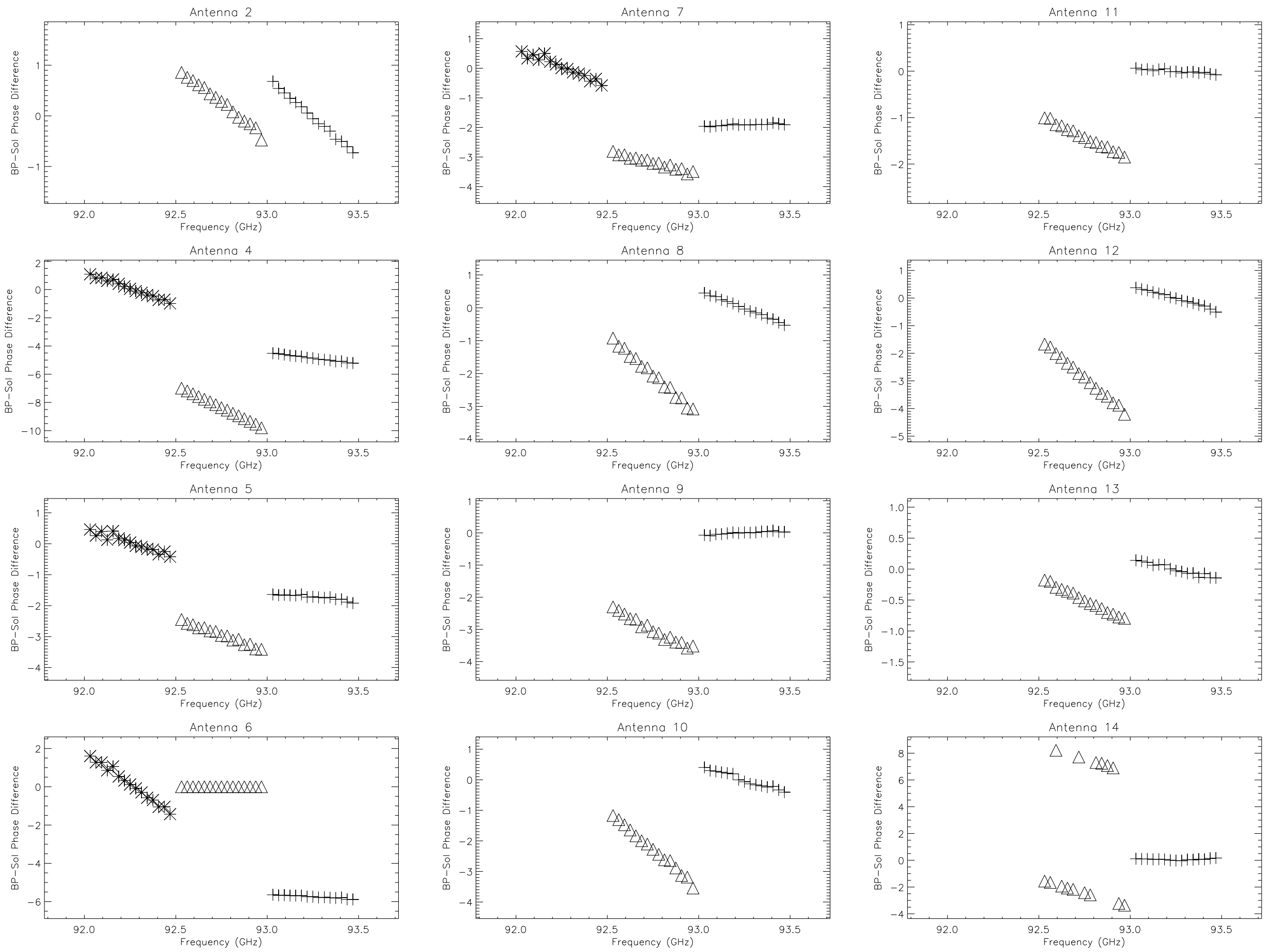

Fig. 14.— The same as Figure 12 for the phase difference of the BP Solutions.

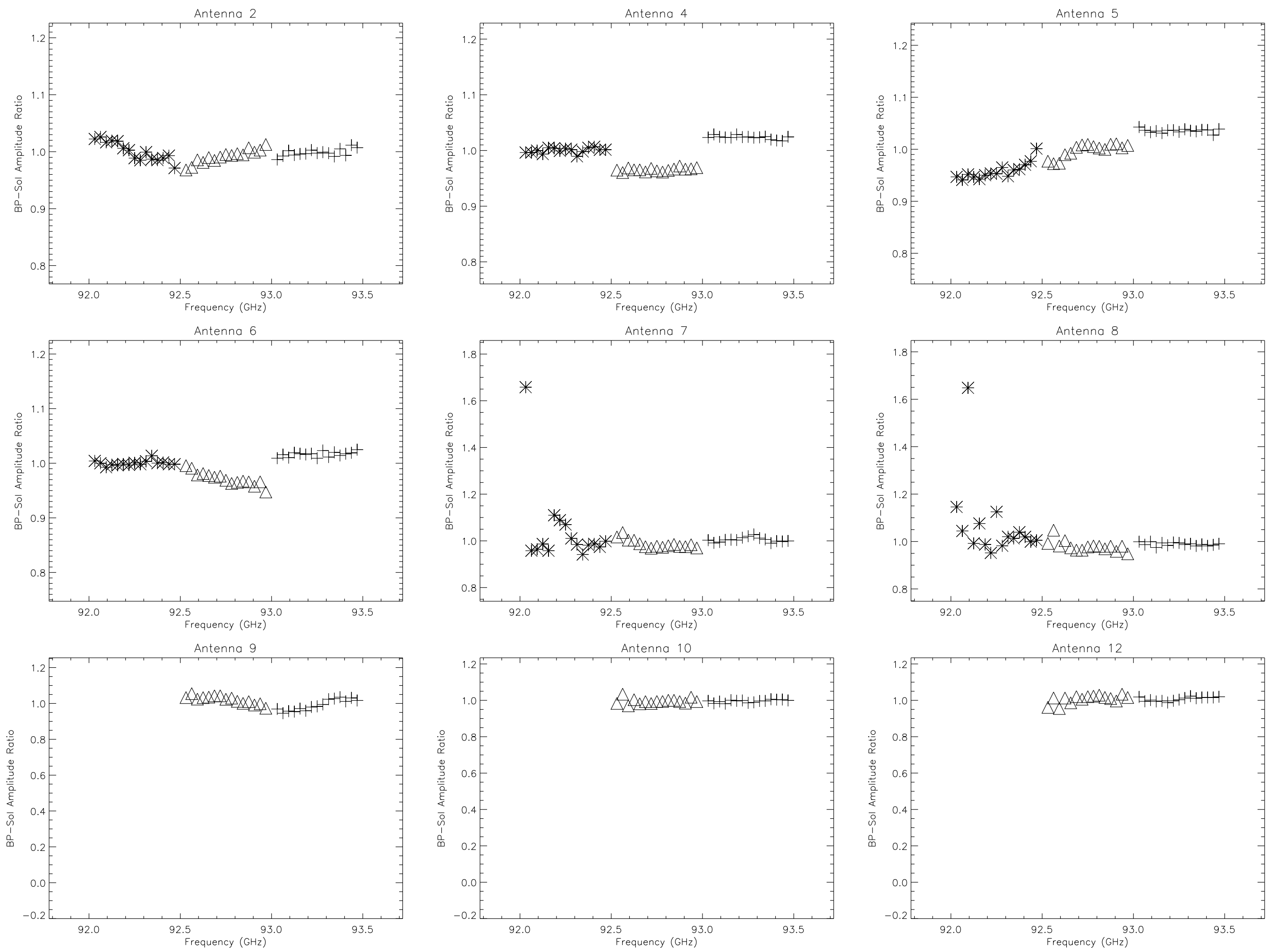

Fig. 15.— Bandpass solutions amplitude ratio between two datasets of the quasar 3c273 taken 6 weeks apart from each other, on 09 Sept 2006 & 20 Oct 2006. We show here example solutions for only 9 antennas. There are only the LSB windows in these dataset and all set at a BW = 500 MHz ($\times$: LSB 1, $+$: LSB 2, $\triangle$: LSB 3). CARMA 1 was the reference antenna on the 09 sep 2006 dataset and CARMA 2 was the reference antenna on the 20 oct 2006 dataset.

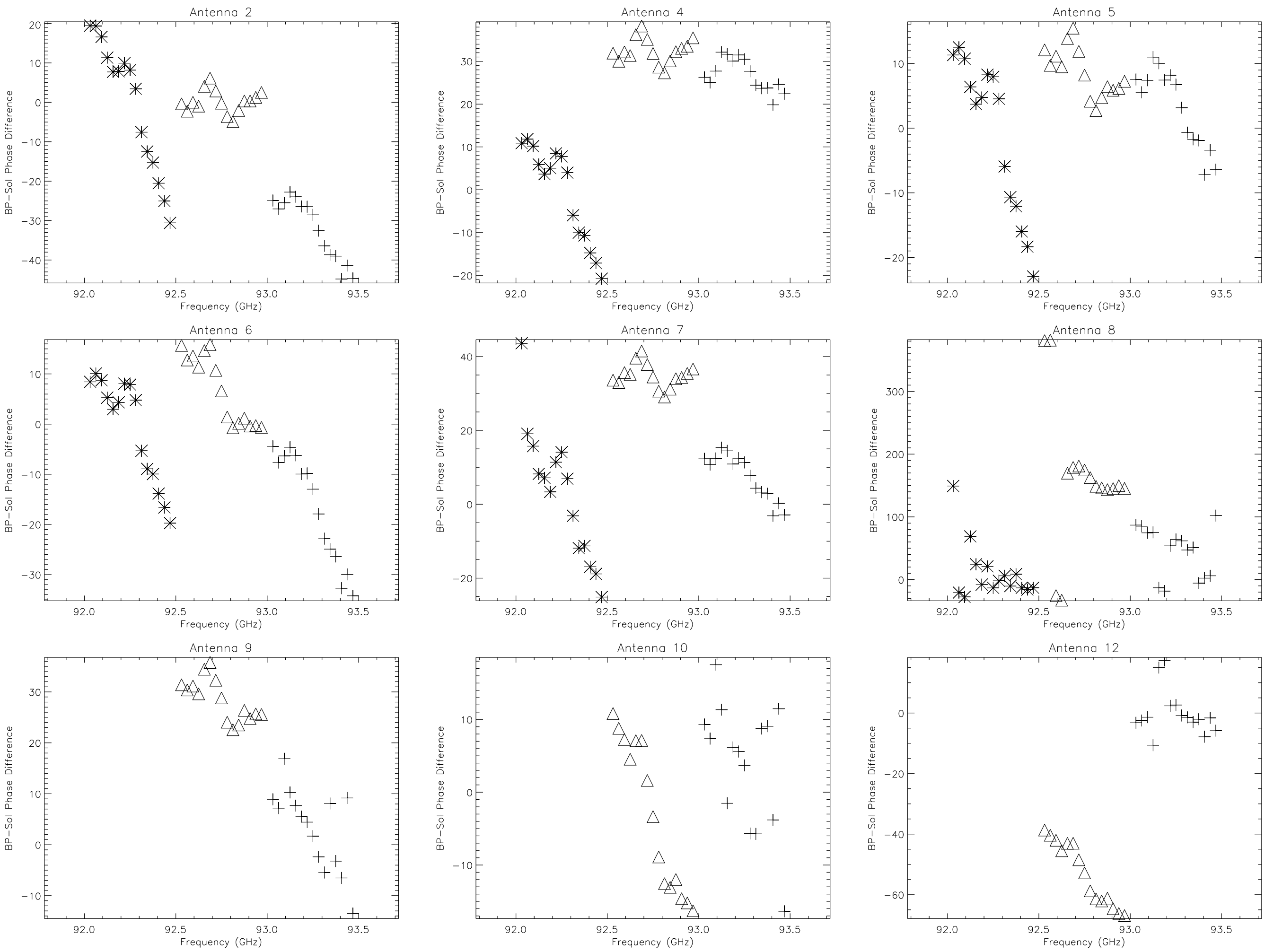

Fig. 16.— The same as Figure 15 for the phase difference of the solutions.